27th EPS Conference on Contr. Fusion and Plasma Phys. Budapest, 12-16 June 2000 ECA Vol. **24B** (2000) 1172 -1175

Comparison of Erosion and Deposition Behaviour of Tungsten and Carbon in the Boundary Plasma of TEXTOR-94

D. Hildebrandt[1], P. Wienhold[2], D. Naujoks[1], W. Schneider[1]

[1] *Max-Planck Institut für Plasmaphysik, Euratom Association, 10117 Berlin, Germany*
[2] *Institut für Plasmaphysik, Forschungszentrum Jülich GmbH, Euratom Association, 52425 Jülich, Germany*

1 Introduction

Post-mortem investigations of outer divertor tiles of ASDEX-Upgrade with plasma facing surfaces of graphite and tungsten have shown distinctly different contamination with deposited plasma species in erosion-dominated areas [1], indicating a different erosion/deposition behaviour of both materials. In fact, the contamination of graphite surfaces has been found to be more than an order of magnitude higher than that observed on tungsten surfaces. A similar observation was made with a graphite-tungsten twin limiter in TEXTOR-94 [2]. Unfortunately, a direct comparison of the deposition behaviour of both materials from all these investigations is difficult because the plasma conditions causing the contamination on the graphite and tungsten surfaces could be different.

In order to compare erosion and deposition effects on tungsten and carbon under equal plasma conditions a polished sample of fine grained graphite with a multi layer coating and plasma facing surfaces of carbon and tungsten was exposed to the scrape-off plasma of TEXTOR-94. The measured erosion and deposition effects are compared with results of an analytical model using simplified assumptions about the sputtering yield for materials with altered homogeneous surface layers [3].

2 Experimental

For the experiment a polished sample of fine grained graphite (size 100 mm · 75 mm · 2 mm) with a tungsten layer of 300 nm thickness was used. This layer was separated from the graphite substrate by a 200 nm thick rhenium layer to avoid diffusion of carbon from the bulk material into the tungsten layer. The major part of the tungsten layer was protected by an amorphous hydrogenated carbon layer (200 nm thick) deposited in a glow discharge in methane (CH_4). Fig.1 shows the original structure of this sample part measured by Secondary Ion Mass Spectrometry prior to the exposure in TEXTOR-94. Two spots with a diameter of 5 mm and locally separated by 22 mm were not protected by the a-C:H film allowing the direct plasma impact on the tungsten layer (fig.2). The specimen was mounted on a graphite probe head and located near the last closed flux surface. Its upper plane was declined by 20^o with respect to the toroidal field and oriented to the ion drift side. A thin Al-shield covered a part of the sample far from the plasma keeping the surface virgin. For further details see ref. [4].

Radial profiles of the plasma density and the electron temperature in the scrape-off layer were measured by the Li- and He-diagnostics [5]. The edge plasma is expected to

be contaminated by carbon with a concentration of a few percent.

After the exposure to 36 NB-heated discharges in TEXTOR-94, with a total exposure time of about 200 s, the surface composition of the sample was investigated using surface analysis techniques with high spatial resolution such as Auger Electron Spectroscopy (AES), Electron Probe Microanalysis (EPMA) and Secondary Ion Mass Spectrometry (SIMS).

3 Results

Fig.3 shows the areal density of carbon and tungsten in dependence on the position across the sample before and after the plasma exposure. These values were obtained by integrating depth profiles measured by AES. The carbon amount of the original a-C:H-layer as measured in the covered area at x = 47 mm was determined to be $1.6 \cdot 10^{22}$ C-atoms m^{-2}. Erosion of the a-C:H-film in the shadowed area (x=65 mm) at the transition from the covered area to the exposed area is due to the impact of neutrals [6]. In the exposed area of the a-C:H-film the carbon density varies between $3 \cdot 10^{22}$ C-atoms m^{-2} (deposition region from x=70 to 90 mm) and $1 \cdot 10^{21}$ C-atoms m^{-2} (region with prevailing erosion for x>100 mm). For the tungsten surface carbon deposition of $6.5 \cdot 10^{21}$ C-atoms m^{-2} was found in spot B at x = 77 mm and $2.5 \cdot 10^{21}$ C-atoms m^{-2} in spot A at x = 97 mm, respectively. Simultaneously occurring erosion caused a loss of about $1.2 \cdot 10^{22}$ W-atoms m^{-2} from the tungsten spot A and $5.5 \cdot 10^{21}$ W-atoms m^{-2} from the spot B, respectively.

The deposition of carbon on the tungsten surface as observed by SIMS-imaging was found to be non-uniform. Fig.4 shows the lateral distribution of carbon in spot A. Analyzing regions of fig.4 with a high carbon SIMS-signal (bright region) we found carbon concentrations up to 65 % by AES whereas regions with a low carbon SIMS-signal (dark region) have a carbon concentration of 35 % only.

4 Discussion

The experimental data presented in table 1 gives evidence of the different deposition behaviour of carbon and tungsten surfaces. They are compared with results from an analytical model [3]. This model describes the erosion/deposition behaviour of multicomponent targets. During the simultaneous bombardment with plasma ions (D^+) and non-recycling impurity ions (C^{n+}) the composition of the exposed tungsten surface changes due to the implantation of the incoming carbon ions. The model considers the growth of a mixed carbon-tungsten layer on the initially clean tungsten surface and the resulting protection effect of this coverage on the tungsten erosion. This contamination is modelled by a homogeneous C-W-layer with an assumed thickness of 7 nm. Carbon deposition causes an increase of its concentration in this layer. The main erosion process for tungsten under the given plasma conditions is physical sputtering by carbon ions. Hence, the concentration of carbon in the plasma edge is a key parameter in the analysis. For carbon removal besides physical sputtering also chemical erosion with a yield of $Y_{chem} = 0.015$ is considered in the analysis.

Describing the present experiment the plasma parameters have been weighted for finding average values for the NBI and ohmic phases. For spot A this yields values of the electron temperature and plasma density of 33 eV and $0.56 \cdot 10^{18}$ m^{-3}, respectively. The corresponding values for spot B were determined to be 30 eV and $0.39 \cdot 10^{18}$ m^{-3}.

	calculated data	**experimental data**
C deposition on C		
near spot A	$2 \cdot 10^{20}$	$3 \cdot 10^{20}$
near spot B	$1.5 \cdot 10^{22}$	$1.3 \cdot 10^{22}$
C deposition on W		
spot A	$4 \cdot 10^{20}$	$2.2 \cdot 10^{21}$
spot B	$7 \cdot 10^{20}$	$6.5 \cdot 10^{21}$
W erosion		
spot A	$3 \cdot 10^{21}$	$1.1 \cdot 10^{22}$
spot B	$1.1 \cdot 10^{21}$	$5.5 \cdot 10^{21}$
C-surface concentration		
spot A	45 %	50 %
spot B	85 %	70 %

Table 1: *Comparison of calculated and measured values in atoms* m^{-2}

Setting the plasma carbon concentration at 3.9% near spot A and 5.8% near spot B then the carbon deposition on the a-C:H layer is satisfactorily described by the model. This is shown in table 1 where the calculated values are presented together with the experimental data obtained as mean values from AES-depth profiling and Electron Probe Microanalysis. In contrast, the calculated values for the C-deposition on tungsten and for the tungsten erosion are considerable lower than the experimental data. This discrepancy can be partly explained by non-uniform carbon deposition and also by carbon diffusion into the tungsten substrate. In fact, both effects have been observed (see fig. 4 and ref. [5]). With the assumption of a pure tungsten surface a simple estimate gives an erosion of about $1 \cdot 10^{22}$ W-atoms m^{-2} from spot A. Taking into account a mean W-concentration of 50 % at the surface (see table 1) this would lead to the erosion of $5 \cdot 10^{21}$ W-atoms m^{-2}. This value agrees somewhat better with the experimental result than that obtained by the model (see table 1).

References

[1] D Hildebrandt et al., J. Nuclear Mater. 266-269(1999)532-537.
[2] M Rubel et al., Physica Scripta T81(1999)61.
[3] D Naujoks et al., J. Nuclear Mater. 230(1996)93.
[4] M Brix, Report of IPP Jülich, Jül-3638(1998).
[5] D Hildebrandt et al., 14th PSI-Conference, Rosenheim 2000.
[6] P Wienhold et al., to be published in Physica Scripta

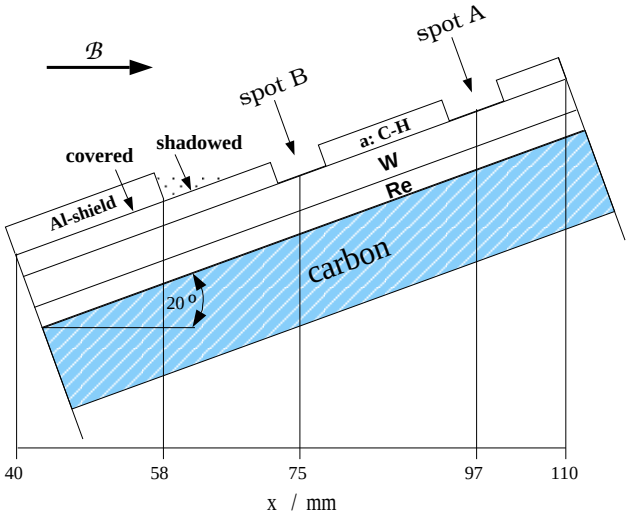

Fig.2 *Arrangement of the multi-layered graphite sample*

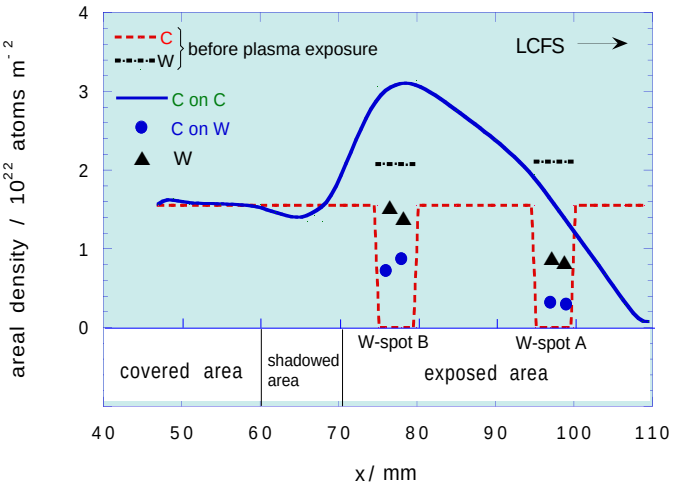

Fig.3 *Areal density of carbon across the sample surface*

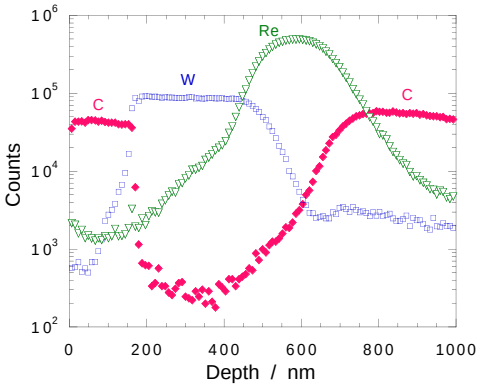

Fig.1 *SIMS-depth profiles from the virgin sample, x=47mm*

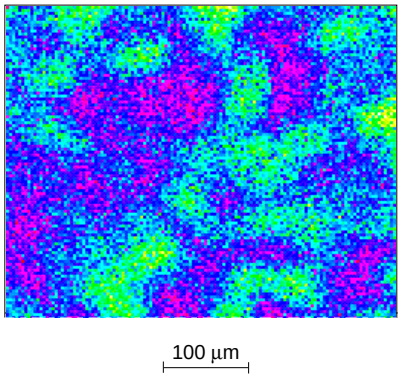

Fig.4 *SIMS-image of the lateral carbon distribution in spot A*